

Phase-controlled pathway interferences and switchable fast-slow light in a cavity-magnon polariton system

Jie Zhao,^{1,2,3,4,*} Longhao Wu,^{1,2,3,*} Tiefu Li,^{5,6} Yu-xi Liu,⁵
Franco Nori,^{7,8} Yulong Liu,^{6,9,†} and Jiangfeng Du^{1,2,3,‡}

¹*Hefei National Laboratory for Physical Sciences at
the Microscale and Department of Modern Physics,
University of Science and Technology of China, Hefei 230026, China*

²*CAS Key Laboratory of Microscale Magnetic Resonance,
University of Science and Technology of China, Hefei 230026, China*

³*Synergetic Innovation Center of Quantum Information and Quantum Physics,
University of Science and Technology of China, Hefei 230026, China*

⁴*National Laboratory of Solid State Microstructures,
School of Physics, Nanjing University, Nanjing 210093, China*

⁵*Institute of Microelectronics, Tsinghua University, Beijing 100084, China*

⁶*Quantum states of matter, Beijing Academy of
Quantum Information Sciences, Beijing 100193, China*

⁷*Theoretical Quantum Physics Laboratory, RIKEN, Saitama, 351-0198, Japan*

⁸*Department of Physics, The University of Michigan,
Ann Arbor, Michigan 48109-1040, USA*

⁹*Department of Applied Physics, Aalto University,
P.O. Box 15100, FI-00076 Aalto, Finland*

(Dated: January 29, 2021)

A. THE DERIVATION OF THE TRANSMISSION SPECTRA

In this section, we derive the detailed expression of transmission spectra in our experiment. We solve the transmission spectra with standard steady state input-output theory. The cavity magnon-polariton system is driven by two beams of microwave, which are called the pump tone and the probe tone. The pump tone is applied through the antenna 2 and drives the magnon with amplitude ε_m and phase φ . In the other side, the probe tone is used as the reference, applied through the antenna 1 and drives the cavity with amplitude ε_c and phase $\varphi_c = 0$. In our setup, the Kittle mode of the YIG sphere is working in the low excitation regime. Using the Holstein-Primakoff transformation, the collective spin mode excitation can be simply regarded as a harmonic oscillator. Therefore, our system can be described with the Hamiltonian

$$\begin{aligned}
 H = & \omega_c a^\dagger a + \omega_m m^\dagger m + g(a^\dagger m + a m^\dagger) \\
 & + i\sqrt{2\eta_c \kappa_c} \varepsilon_c (a^\dagger e^{-i\omega_p t} - a e^{i\omega_p t}) \\
 & + i\sqrt{2\eta_m \kappa_m} \varepsilon_m (m^\dagger e^{-i\omega_p t - i\varphi} - m e^{i\omega_p t + i\varphi}). \tag{S1}
 \end{aligned}$$

Here, we have assumed $\hbar = 1$. a (a^\dagger) and m (m^\dagger) are the annihilation (creation) operator of the cavity with resonant frequency ω_c and the magnon mode with resonant frequency ω_m , respectively. κ_c and κ_m are the decay rates of the cavity and the magnon mode, respectively. We define the coupling parameter of the cavity (the magnon mode) as $\eta_c = \kappa_{c1}/\kappa_c$ ($\eta_m = \kappa_{m1}/\kappa_m$), where κ_{c1} and κ_{m1} are the external dissipation rates of the cavity and the magnon, respectively. In our experiment, the coupling parameter of the cavity is $\eta_c = 0.19$ which is less than $1/2$, and the cavity works in under coupling regime. Mean while, the coupling parameter of the magnon mode is $\eta_m = 1/2$, and the magnon works in the critical coupling regime. $\varepsilon_c = \sqrt{P_c/\omega_p}$ ($\varepsilon_m = \sqrt{P_m/\omega_p}$) is the amplitude of the cavity probe (the magnon pump) field. Where P_c (P_m) is the power of cavity probe (magnon pump) tone. ω_p is the frequency of the cavity probe tone, and is equal to the frequency of the magnon pump tone. φ is the relative phase between the cavity probe tone and the magnon pump tone. Moving to the reference frame rotating with frequency ω_p , we can write the Hamiltonian as:

* These authors contributed equally to this work

† liuy1@baqis.ac.cn

‡ djf@ustc.edu.cn

$$\begin{aligned}
H &= \Delta_p a^\dagger a + \Delta_p m^\dagger m + g(a^\dagger m + a m^\dagger) \\
&\quad + i\sqrt{2\eta_c \kappa_c} \varepsilon_c (a^\dagger - a) + i\sqrt{2\eta_m \kappa_m} \varepsilon_m (m^\dagger e^{-i\varphi} - m e^{i\varphi}),
\end{aligned} \tag{S2}$$

where $\Delta_p = \omega_c - \omega_p$ ($\Delta_p = \omega_m - \omega_p$) is the detuning between cavity resonant frequency (magnon mode resonant frequency) and probe (pump) tones. In our setup, the cavity is resonant with the magnon mode, i.e. $\omega_c = \omega_m$. The dynamics of the cavity magnon-polariton system can be described by solving the corresponding semiclassical Langevin equations:

$$\dot{a} = -(i\Delta_p + \kappa_c) a - igm + \sqrt{2\eta_c \kappa_c} \varepsilon_c, \tag{S3}$$

$$\dot{m} = -(i\Delta_p + \kappa_m) m - iga + \sqrt{2\eta_m \kappa_m} \varepsilon_m e^{-i\varphi}. \tag{S4}$$

For steady states, we can obtain the solution of $\langle a \rangle$ and $\langle m \rangle$:

$$\begin{aligned}
\langle a \rangle &= \frac{\sqrt{2\eta_c \kappa_c} \varepsilon_c (i\Delta_p + \kappa_m)}{(i\Delta_p + \kappa_c)(i\Delta_p + \kappa_m) + g^2} - \frac{ig\sqrt{2\eta_m \kappa_m} \varepsilon_m e^{-i\varphi}}{(i\Delta_p + \kappa_c)(i\Delta_p + \kappa_m) + g^2}, \\
\langle m \rangle &= \frac{-ig\langle a \rangle + \sqrt{2\eta_m \kappa_m} \varepsilon_m e^{-i\varphi}}{i\Delta_p + \kappa_m}.
\end{aligned} \tag{S5}$$

The reflected signal from the cavity follows the input-output boundary condition

$$\varepsilon_{\text{out}} = \varepsilon_c - \sqrt{2\eta_c \kappa_c} \langle a \rangle. \tag{S6}$$

Using the input-output boundary condition, we can solve the reflection coefficient as

$$\begin{aligned}
t &= \frac{\varepsilon_{\text{out}}}{\varepsilon_c} \\
&= 1 - \frac{2\eta_c \kappa_c (i\Delta_p + \kappa_m)}{(i\Delta_p + \kappa_c)(i\Delta_p + \kappa_m) + g^2} + \frac{i2g\sqrt{\eta_c \eta_m \kappa_c \kappa_m} \delta e^{-i\varphi}}{[(i\Delta_p + \kappa_c)(i\Delta_p + \kappa_m) + g^2]} \\
&= t_{\text{probe}} + t_{\text{pump}},
\end{aligned} \tag{S7}$$

where $t_{\text{probe}} = 1 - \frac{2\eta_c \kappa_c (i\Delta_p + \kappa_m)}{(i\Delta_p + \kappa_c)(i\Delta_p + \kappa_m) + g^2}$, $t_{\text{pump}} = \frac{ig\sqrt{2\eta_c \kappa_c} \sqrt{2\eta_m \kappa_m} \delta e^{-i\varphi}}{(i\Delta_p + \kappa_c)(i\Delta_p + \kappa_m) + g^2}$, and $\delta = \varepsilon_m / \varepsilon_c$ is the pump-probe ratio. Using the reflection coefficient, we can obtain the amplitude response spectrum S_{11} by

$$S_{11} = |t| \quad (\text{S8})$$

Meanwhile, we can also obtain the phase of the reflected signal by

$$\varphi = \arg(t). \quad (\text{S9})$$

Using the definition of group delay of microwave, $\tau_d = \partial\varphi/\partial\omega_p$, we can obtain the group delay time of the transmitted microwave at the resonant frequency,

$$\tau_{d0} = - \left. \frac{\partial\varphi}{\partial\Delta_p} \right|_{\Delta_p=0} \quad (\text{S10})$$

B. THE SIDE-EFFECT OF THE ANTENNA 2

In our experiment, the round loop antenna 2 is not only coupled to the magnon mode but also to the cavity mode. The redundant coupling introduces another input-output port to the cavity, and induces an additional dissipation rate κ_{c2} of the cavity. Therefore, the pump tone we applied to the magnon also drives the cavity. In this section, we inspect the effects of this auxiliary coupling, and compare the transmission spectra and group delay time with that without the influence of dissipation rate κ_{c2} .

With the existence of the antenna 2, the Hamiltonian of our system can be written as

$$\begin{aligned} H = & \omega_c a^\dagger a + \omega_m m^\dagger m + g(a^\dagger m + a m^\dagger) \\ & + i\sqrt{2\eta_c \kappa_c} \varepsilon_c (a^\dagger e^{-i\omega_p t} - a e^{i\omega_p t}) \\ & + i\sqrt{2\eta_m \kappa_m} \varepsilon_m (m^\dagger e^{-i\omega_p t - i\varphi} - m e^{i\omega_p t + i\varphi}) \\ & + i\sqrt{2\kappa_{c2}} \varepsilon_m (a^\dagger e^{-i\omega_p t - i\varphi_2} - a e^{i\omega_p t + i\varphi_2}). \end{aligned} \quad (\text{S11})$$

Where κ_{c2} is the antenna 2 induced cavity decay rate, and φ_2 is the relative phase between the pump tone and the probe tone applied to the cavity. In the reference frame rotating with angular frequency ω_p , the Hamiltonian is

$$\begin{aligned} H = & \Delta_p a^\dagger a + \Delta_p m^\dagger m + g(a^\dagger m + a m^\dagger) + i\sqrt{2\eta_c \kappa_c} \varepsilon_c (a^\dagger - a) \\ & + i\sqrt{2\eta_m \kappa_m} \varepsilon_m (m^\dagger e^{-i\varphi} - m e^{i\varphi}) + i\sqrt{2\kappa_{c2}} \varepsilon_m (a^\dagger e^{-i\varphi_2} - a e^{i\varphi_2}). \end{aligned} \quad (\text{S12})$$

Using the semiclassical Langevin equations, we can solve the steady state internal field of the magnon and the cavity as:

$$\begin{aligned}
a &= \frac{\sqrt{2\eta_c\kappa_c}\varepsilon_c(i\Delta_p + \kappa_m)}{(i\Delta_p + \kappa_c)(i\Delta_p + \kappa_m) + g^2} - \frac{ig\sqrt{2\eta_m\kappa_m}\varepsilon_m e^{-i\varphi}}{(i\Delta_p + \kappa_c)(i\Delta_p + \kappa_m) + g^2} \\
&\quad + \frac{\sqrt{2\kappa_c2}\varepsilon_m(i\Delta_p + \kappa_m) e^{-\varphi_2}}{(i\Delta_p + \kappa_c)(i\Delta_p + \kappa_m) + g^2}, \\
m &= \frac{-iga + \sqrt{2\eta_m\kappa_m}\varepsilon_m e^{-i\varphi}}{i\Delta_p + \kappa_m}.
\end{aligned} \tag{S13}$$

The antenna 2-cavity coupling does not change the input-output boundary condition which is described in Eq. (S6). Therefore, the reflection coefficient can be expressed as

$$\begin{aligned}
t &= \frac{\varepsilon_{\text{out}}}{\varepsilon_c} \\
&= 1 - \frac{2\eta_c\kappa_c(i\Delta_p + \kappa_m)}{(i\Delta_p + \kappa_c)(i\Delta_p + \kappa_m) + g^2} + \frac{i2g\sqrt{\eta_c\eta_m\kappa_c\kappa_m}\varepsilon_m e^{-i\varphi_m}}{\varepsilon_c [(i\Delta_p + \kappa_c)(i\Delta_p + \kappa_m) + g^2]} \\
&\quad - \frac{2\sqrt{\eta_c\kappa_c\kappa_c2}\varepsilon_m(i\Delta_p + \kappa_m) e^{-\varphi_2}}{\varepsilon_c [(i\Delta_p + \kappa_c)(i\Delta_p + \kappa_m) + g^2]}.
\end{aligned} \tag{S14}$$

Using the Eq. (S8) and Eq. (S10), we can obtain the amplitude response spectra S_{11} and the group delay time τ_d with considering the side-effects of the antenna 2. To evaluate the influence of the antenna 2-cavity coupling on the transmission properties, we compare the amplitude response spectra S_{11} and the group delay time calculated using Eq. (S7) and Eq. (S14).

In Fig. S1, we plot the main theoretical results of amplitude response spectra and the group delay time with and without considering the effects of antenna 2-cavity coupling. In Fig. S1(a), we compare the reflection spectrum S_{11} with the applied microwave phase 0.35π . And in Fig. S1(b), we compare the group delay time with the same applied microwave phase. In Fig. S1(c) and (d), we compare the extreme amplitude of S_{11} calculated with different pump-probe ratio δ when the applied microwave phase is 0.35π and 1.35π , respectively. In Fig. S1(e) and (f), we compare the extreme amplitude of the group delay time solved with various δ when the applied microwave phase is 0.35π and 1.35π , respectively. We can find from these comparisons that the impacts of the antenna 2-cavity coupling on the system responses are trivial. Therefore, we can use the physical model described in the main text to explain the experiment results in our manuscript. In order to fit the experimental results better, we considered the effects of antenna 2-cavity coupling in theoretical results presented in the main text.

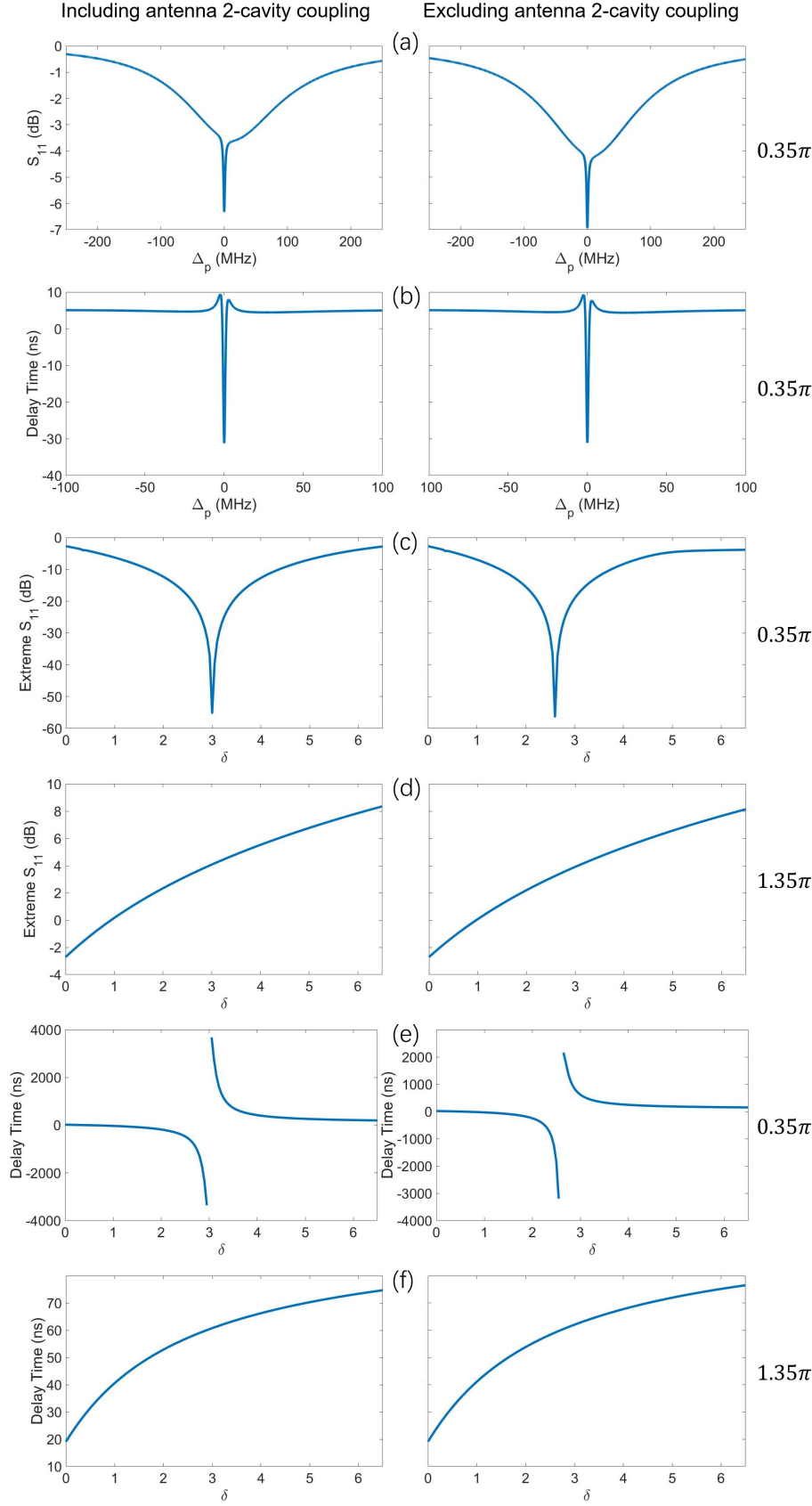


FIG. S1. Comparisons of the system responses with and without the impacts of antenna 2-cavity coupling. Here, the applied microwave phase φ is presented by the experimental parameter. Theoretically, the fitted values of φ (φ_2) are 1.5π (0.8π) and 0.4π (1.4π) when the experimental values are 0.35π and 1.35π , respectively. (a) The amplitude responses with $\delta = 1$ and the applied microwave phase $\varphi = 0.35\pi$. (b) The group delay time with $\delta = 1$ and the applied microwave phase $\varphi = 0.35\pi$. (c) Extreme values of the amplitude responses S_{11} with different pump-probe ratio δ and applied microwave phase $\varphi = 0.35\pi$. (d) Extreme values of the amplitude responses S_{11} with different pump-probe ratio δ and applied microwave phase $\varphi = 1.35\pi$. (e) Extreme values of the group delay time with different pump-probe ratio δ and applied microwave phase $\varphi = 0.35\pi$. (f) Extreme values of the group delay time with different pump-probe ratio δ and applied microwave phase $\varphi = 1.35\pi$.

C. ERROR ANALYSIS

In Fig.5(a) of the main text, we can find that the experimental data deviates from the theoretical result around the abrupt transition point. This is mainly induced by the imperfect system setups, such as limited output precision of AWG, imperfectness of the IQ mixer and unstable magnon frequency. We give the detailed discussions below.

Besides the 2D curves shown in Fig5 (a), we also provide 3D figures here to present how group delay time evolutions versus both the pump-probe ratio δ and the sweep step of the detuning frequency Δ_p , as shown in Fig. S2. Fig. S2(a) presents the theoretical results obtained with our system parameters, and Fig. S2(b) is the experimental result. The step of pump-probe amplitude ratio δ is 0.053 and the step of the detuning frequency Δ_p is 60 kHz. We can find that the experimental data present the same behavior with the theoretical calculations. However, the experimental data deviates from the theoretical result around the transition point ($\delta = 3, \Delta_p = 0$).

In order to present the parameter sensitivity of the delay time around the transition point, lets zoom in and calculate the delay time around this point by refining the sweep step. As shown in Fig. S2(c)-(f), the extreme value of the delay time increases sharply with further decreasing the coordinate step size. As shown in figure (f), when the sweep step for frequency detuning Δ_p is 1 mHz (0.001Hz) and the step of δ is 1×10^{-9} , the maximum delay time reaches 200 s. With further refinement, the extreme value approaches 40000s, which are not presented here due to the great difficulties in experimental realization. From these calculations, we can conclude that the extreme values of delay time increase sharply and the theoretical delay time does approaches infinity.

It is notable that the time delay value is quite sensitive to the sweep step changes (both δ and Δ_p). In our experiment, the amplitude ratio δ is dominated by the output precision of AWG and IQ mixer, and the step is set to be 0.053. This step size corresponds to the finest output precision of AWG. Considering the imperfectness of the IQ mixer, we can expect that the deviation between the set value of δ and the actual one is in the order of 0.01. On the other side, there are current fluctuations of our electromagnet supply. The current fluctuation results the magnon frequency drift in the order of 100 kHz. The frequency drift leads to the frequency detuning between the magnon and the cavity, as well as imprecise step size of Δ_p . We find from our calculations that the variation of delay time reaches $2 \mu\text{s}$ with changing Δ_p 60kHz in the vicinity of the transition point. These factors together cause the measured time delay to be smaller than the theoretical one in the vicinity of the abrupt transition point. Based on the above discussions, it is reasonable that

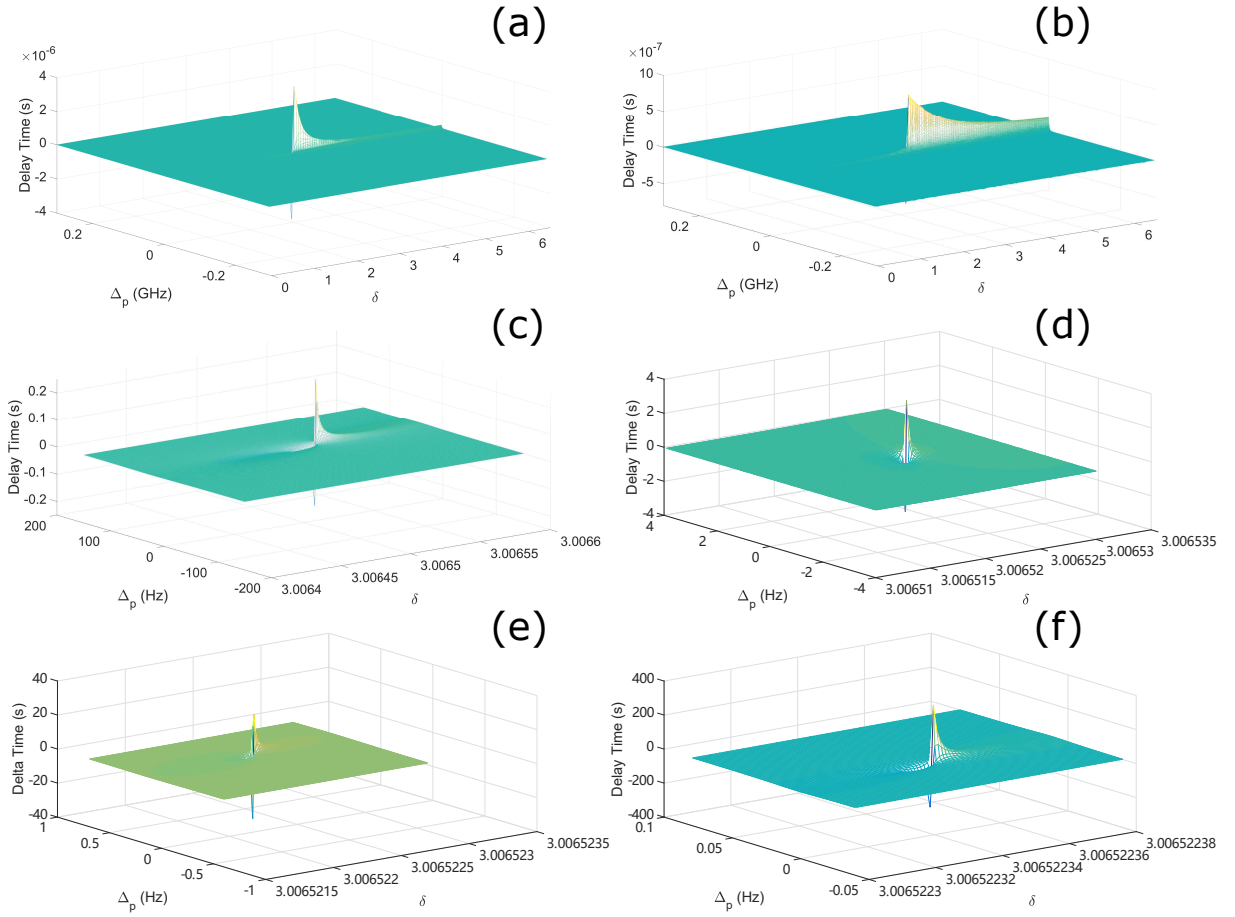


FIG. S2. (a) The theoretical data obtained with experimental parameters (the step of δ is 0.053 and the step of driving frequency is 0.06 MHz). (b) The experimental data. (c) The theoretical data obtained with the step of δ is 1×10^{-6} and the step of driving frequency is 1 Hz. (d) The theoretical data obtained with the step of δ is 1×10^{-7} and the step of driving frequency is 0.1 Hz. (e) The theoretical data obtained with the step of δ is 1×10^{-8} and the step of driving frequency is 0.01 Hz. (f) The theoretical data obtained with the step of δ is 1×10^{-9} and the step of driving frequency is 0.001 Hz.

the measured maximum group delay time (800 ns) deviates from the theoretical one (3.8 μ s).